Deep Resources Engineering 3 (2026) 100202

Contents lists available at ScienceDirect

Deep Resources Engineering

journal homepage: www.keaipublishing.com/en/journals/deepre/

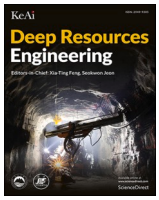

Full length article

Multidimensional thorough perception system for surrounding rock disasters in underground engineering and its application

Haoyu Mao [a], Nuwen Xu [a,*], Peiwei Xiao [a], Xiang Zhou [a,b], Xinchao Ding [c], Biao Li [d]

[a] State Key Laboratory of Hydraulics and Mountain River Engineering, College of Water Resource and Hydropower, Sichuan University, Chengdu 610065, China
[b] CHN Energy Dadu River Hydropower Development Co., Ltd., Chengdu 610041, China
[c] PowerChina Northwest Engineering Co., Ltd., Xi'an 710065, China
[d] School of Geoscience and Technology, Southwest Petroleum University, Chengdu 610500, China

ARTICLE INFO

Keywords:
Underground engineering
Advanced geological prediction
MS monitoring
Multidimensional thorough perception system
Precursory information

ABSTRACT

The excavation process in large underground engineering projects faces the challenges of various disasters, and safety monitoring is an important method for addressing these challenges. To ensure the construction safety of the underground powerhouse at the Jinchuan hydropower station, a multidimensional monitoring system was established. On the basis of a collapse accident during the construction process, early warning precursor information was summarized and successfully applied to the surge chamber. (1) A "point, line, plane, and body" multidimensional thorough perception system that is based on conventional monitoring, a tunnel geology survey (TGS) 360 Pro system, seismic wave CT, and microseismic (MS) monitoring was established. "Point and line" conventional monitoring was used for long-term stability monitoring, "plane" monitoring was used to delineate potential risk areas for subsequent excavations, and "body" monitoring was used to strengthen the monitoring of risk areas. (2) Through the collapse of the roof arch at the underground powerhouse, the MS precursory information of the surrounding rock disaster was analysed, and the results are summarized as follows: the number of MS events, cumulative energy and magnitude increased suddenly; the b value and centre frequency decreased; the apparent stress increased suddenly to a large value and then decreased suddenly; and the cumulative apparent volume increased steeply. (3) A multidimensional system was applied to the surge chamber, and the deformation of the surrounding rock was successfully monitored. Corresponding measures were taken to avoid losses of life and property, which indicates the effectiveness of the multidimensional system. The results of this study can provide a reference for similar underground engineering excavations and disaster protection.

1. Introduction

As the world's largest renewable clean energy source, hydropower plays an important role in promoting the transformation of China's energy structure. China's hydropower projects are distributed mainly in the southwest region. Owing to the complex topography of the southwestern region, these hydropower projects are usually arranged underground. Affected by complex geological conditions and strong excavation unloading, instability of the surrounding rock at underground caverns is easily induced, which poses great challenges to the safe construction of underground engineering [1–3]. During the excavation of the Jinping I hydropower station, a series of surrounding rock instability phenomena occurred: The large deformation at the downstream spandrel of the transformer chamber exceeded 200 mm, and cracking occurred throughout the entire downstream spandrel at the main powerhouse. When the excavation reached the sixth floor, the depth of the rock loose zone exceeded 17 m, and approximately 40 % of the anchor cables were stressed beyond the design value [4]. Owing to the poor interlocking of thin strata, collapse accidents occur frequently in the excavation process of diversion tunnels and large underground caverns at the Wudongde hydropower station [5–9]. Owing to the influence of the weak interlayer zone, the underground powerhouses on the left and right banks of the Baihetan hydropower station have repeatedly collapsed, with lengths of nearly 10 m and depths of 1 m, which seriously endangers construction safety [10–16]. The Shuangjiangkou hydropower station is affected by high in situ stress. During the

Peer review under responsibility of Editorial Board of of Deep Resources Engineering.
* Corresponding author.
E-mail address: xunuwen@scu.edu.cn (N. Xu).

https://doi.org/10.1016/j.deepre.2025.100202
Received 8 April 2025; Received in revised form 4 June 2025; Accepted 30 June 2025
Available online 2 July 2025

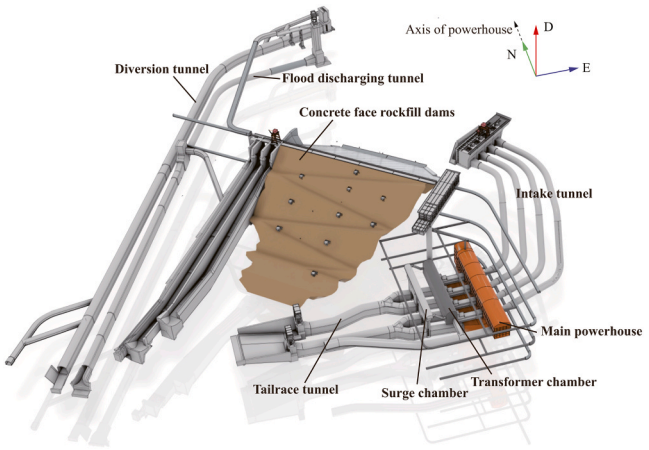

Fig. 1. The overall layout of Jinchuan hydropower station [49].

excavation and unloading processes for the underground powerhouse, the access tunnel, and the tailrace tunnel, several collapse and rock burst accidents have occurred, which have resulted in serious construction delays [17–19]. In addition to the hydropower field, many projects, such as pumped storage projects [20], nuclear waste disposal [21,22], oil and gas storage [23–25], traffic tunnels [26–29], and underground mining [30–34], have surrounding rock instability due to complex geological conditions, which restricts construction safety.

The above surrounding rock instability accidents seriously affect the safety and progress of the projects. To ensure the safe and efficient excavation of underground caverns, safety monitoring is particularly important. Scholars have conducted many studies on various monitoring methods [35,36]. Wang et al. [37] monitored the whole process of splitting failure at the Dagangshan underground cavern through a borehole TV and a micrometer. Li et al. [38–40] adopted microseismic (MS) monitoring systems at the Wudongde hydropower station and Houziyan hydropower station, established a relationship between the construction state and MS activity, and revealed the key factors that cause surrounding rock damage by combining a multipoint displacement meter and an anchor rod stress meter. Dai et al. [41]; Xiao et al. [42,43]; and Zhao et al. [44,45] installed MS sensors in large underground caverns at the Baihetan hydropower station to capture the microfracture information of rock masses, evaluated the stability of underground caverns during excavation and unloading, and revealed the surrounding rock failure mechanism using a multipoint displacement meter and a borehole TV. Mao et al. [46] used the engineering analogy method to predict the surrounding rock deformation of the Lianghekou underground powerhouse by summarizing the abnormal monitoring data before the instability of similar hydropower projects and solved the problem of the inability to monitor the surrounding rock because of damage to the monitoring instrument. Xue and Xiao [47] analysed the monitoring data from 36 sets of multipoint displacement meters installed in the underground caverns of the Xiangjiaba hydropower station. A PSO–LSSVM machine learning model was proposed for predicting the deformation of the surrounding rock during the excavation of underground caverns by considering the geological conditions, locations of the monitoring instruments and space–time conditions before and after measuring the input parameters and surrounding rock deformation as the output parameters. Through a comprehensive monitoring system for underground caverns, Li et al. [48] clarified the deformation characteristics of the weak interlayer zone, determined the failure mode of the rock mass within the weak interlayer zone, and guided support design and optimization.

Although various monitoring measures have been adopted in the construction of underground caverns in hydropower projects to monitor the instability of surrounding rock, they are usually “point” and “line” monitoring methods, such as monitoring by multipoint displacement meters, bolt stress meters, and borehole TVs. These monitoring methods usually have spatial limitations and time lags and cannot guarantee the safety of the whole project. In light of this, Sect. 2 provides an overview of the engineering background and geological conditions and then presents a detailed analysis of the roof arch collapse disaster at the main powerhouse of the Jinchuan hydropower station. On the basis of conventional monitoring methods, Sect. 3 introduces TGS 360 Pro, seismic wave CT and MS monitoring to conduct an in-depth analysis of the monitoring results, summarizes the precursory warning information before the surrounding rock disaster, and constructs a multidimensional thorough perception system of type “point, line, plane, and body”. Sect. 4 applies the multidimensional perception system to the surge chamber, captures the precursor of surrounding rock instability, and adjusts the support measures in time to effectively prevent the further development of surrounding rock deformation.

2. Engineering background

2.1. Engineering overview and geological conditions

The Jinchuan hydropower station is located in Jinchuan County, Aba Tibetan and Qiang Autonomous Prefecture, Sichuan Province. It is the

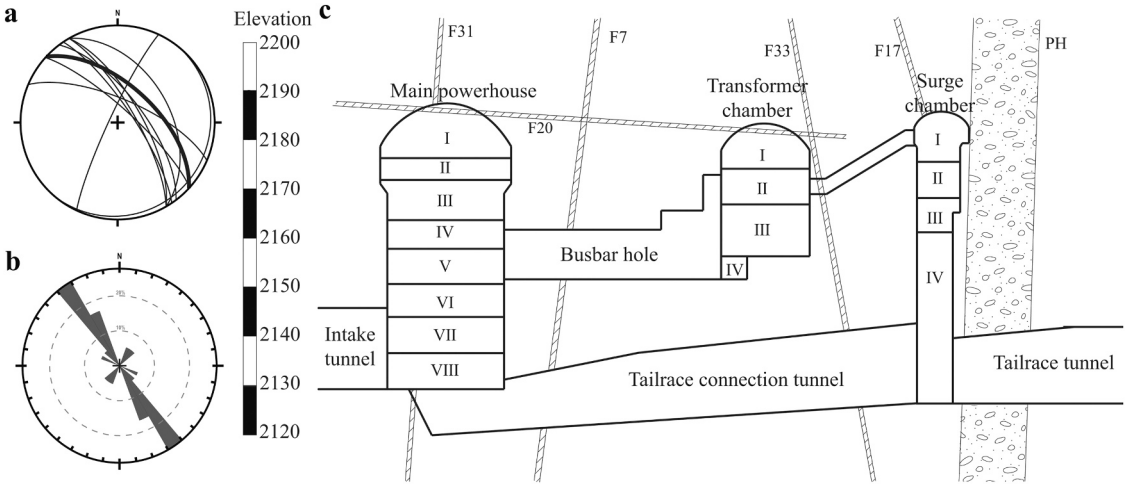

Fig. 2. Section view of water diversion power generation system: (a) Stereographic projection of geological structures (Reproduced from [49]); (b) Rose diagram of geological structure; (c) Geological profile of Jinchuan underground powerhouse.

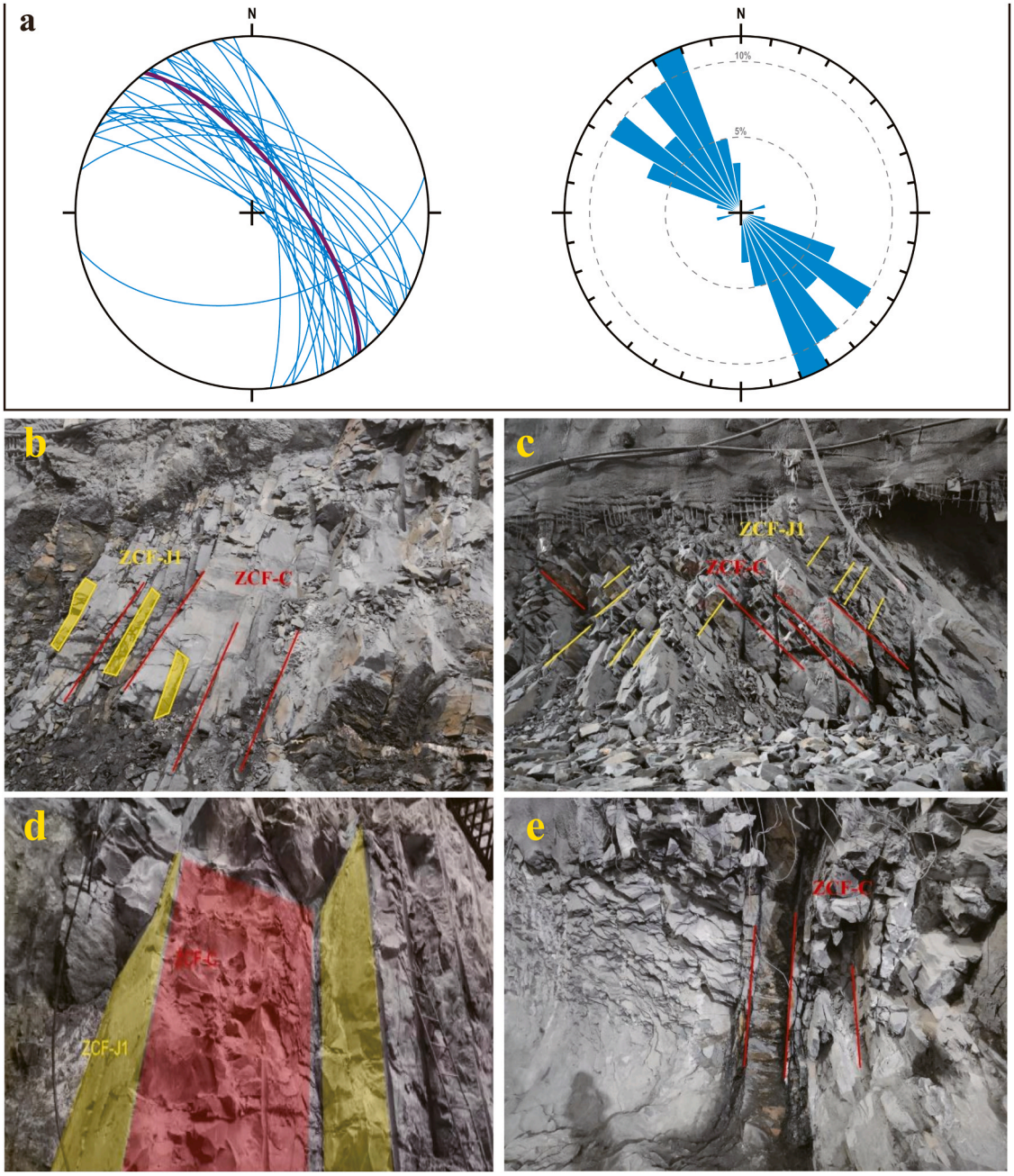

Fig. 3. The faults after excavation exposure: (a) Stereo-plane projection and rose joint diagram of large faults; (b) Stereo-plane projection and rose joint diagram of small faults; (c-f) Photos of faults.

sixth cascade hydropower station in the Dadu River basin and connects with the Shuangjiangkou hydropower station upstream and the Badi hydropower station below. The total installed capacity of the power station is 900 MW, and the annual average power generation capacity of the joint operation with the Shuangjiangkou hydropower station is 3.546 billion kWh.

The Jinchuan hydropower station consists of a river-blocking dam, a left bank water diversion power generation system, a right bank diversion tunnel, an ecological drainage channel, and a spillway tunnel. The river-blocking dam is a concrete face rockfill dam with a maximum height of 112 m. It is placed on the overburden layer with a maximum thickness of approximately 65 m. It is the deepest overburden face rockfill dam under construction, and its construction is difficult.

The water diversion and power generation system is arranged in the mountain on the left bank and is composed of a water inlet, intake tunnel, underground powerhouse, transformer chamber, surge chamber, and tailrace tunnel, among other components. Four generator sets are arranged in the underground powerhouse, with a size of 162 m × 24.8 m × 62.8 m (length × width × height). The transformer chamber is 125 m × 16.5 m × 25.2 m (length × width × height), the surge chamber is 113.65 m × 10.20 m × 52 m (length × width × height), and the following tailrace tunnel adopts the layout of “two machines and one tunnel”. The overall layout of the Jinchuan hydropower station is shown in Fig. 1. The water diversion and power generation system is excavated via layered excavation. The main powerhouse has eight layers, the main transformer chamber and the surge chamber are excavated in four layers, and the excavation profile of the three caverns is shown in Fig. 2.

The stratum lithology in the dam site area is layered metamorphic fine sandstone with carbonaceous phyllite, and the rock mass is relatively broken. The geological structure is relatively simple and is

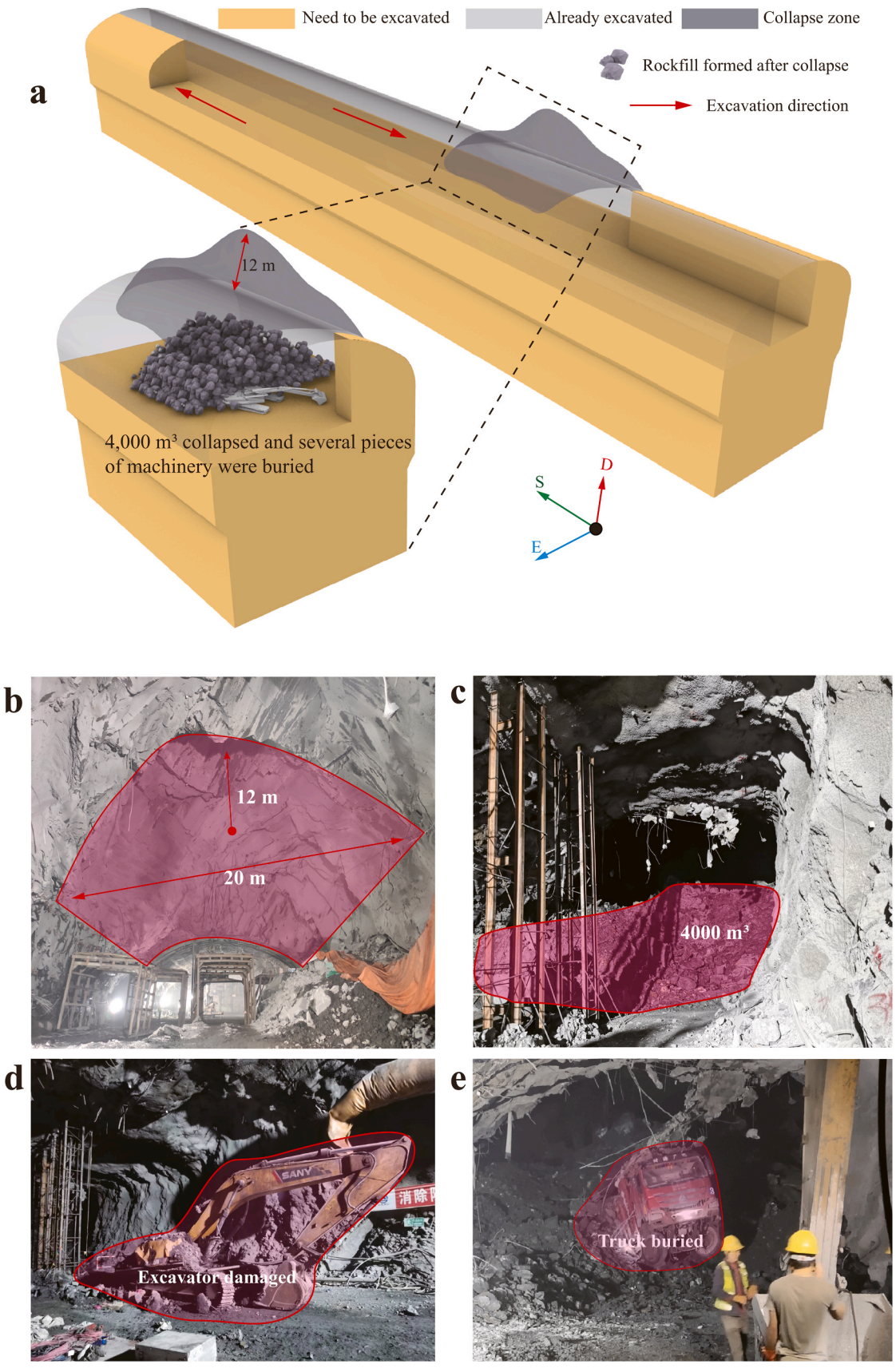

Fig. 4. The schematic diagram of the collapse and the photos: (a) Disaster location and excavation condition; (b) More than 12 m deep pit; (c) More than 4000 cubic meters of collapse; (d) Excavators buried; (e) Truck buried (Reproduced from [49]).

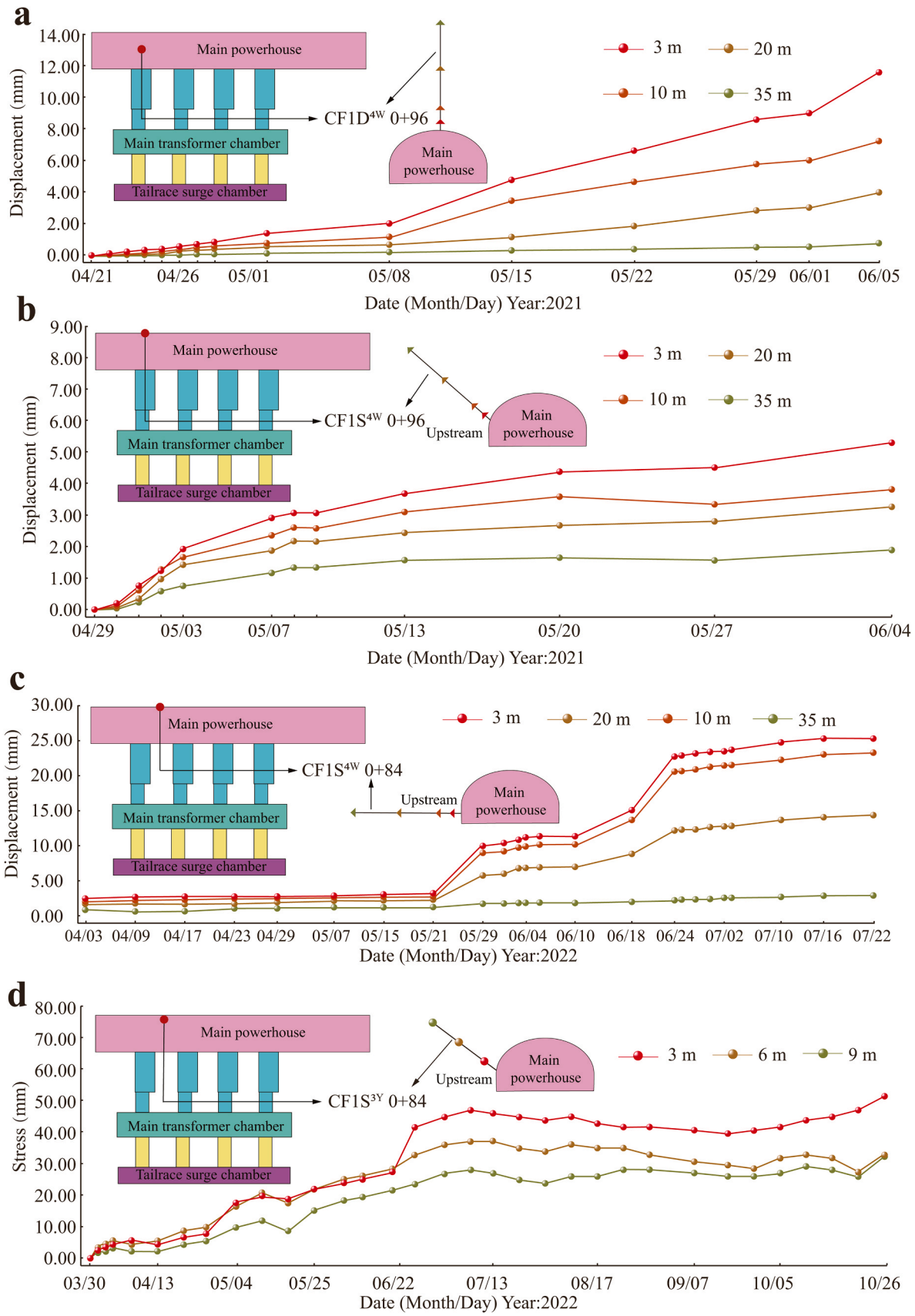

Fig. 5. "Point" monitoring results: (a) Multi-point displacement meter of 0 + 96 m top arch; (b) Multi-point displacement meter of 0 + 96 upstream spandrel; (c) Multi-point displacement meter of 0 + 84 m upstream side wall; (d) Bolt stress meter of 0 + 84 m upstream spandrel.

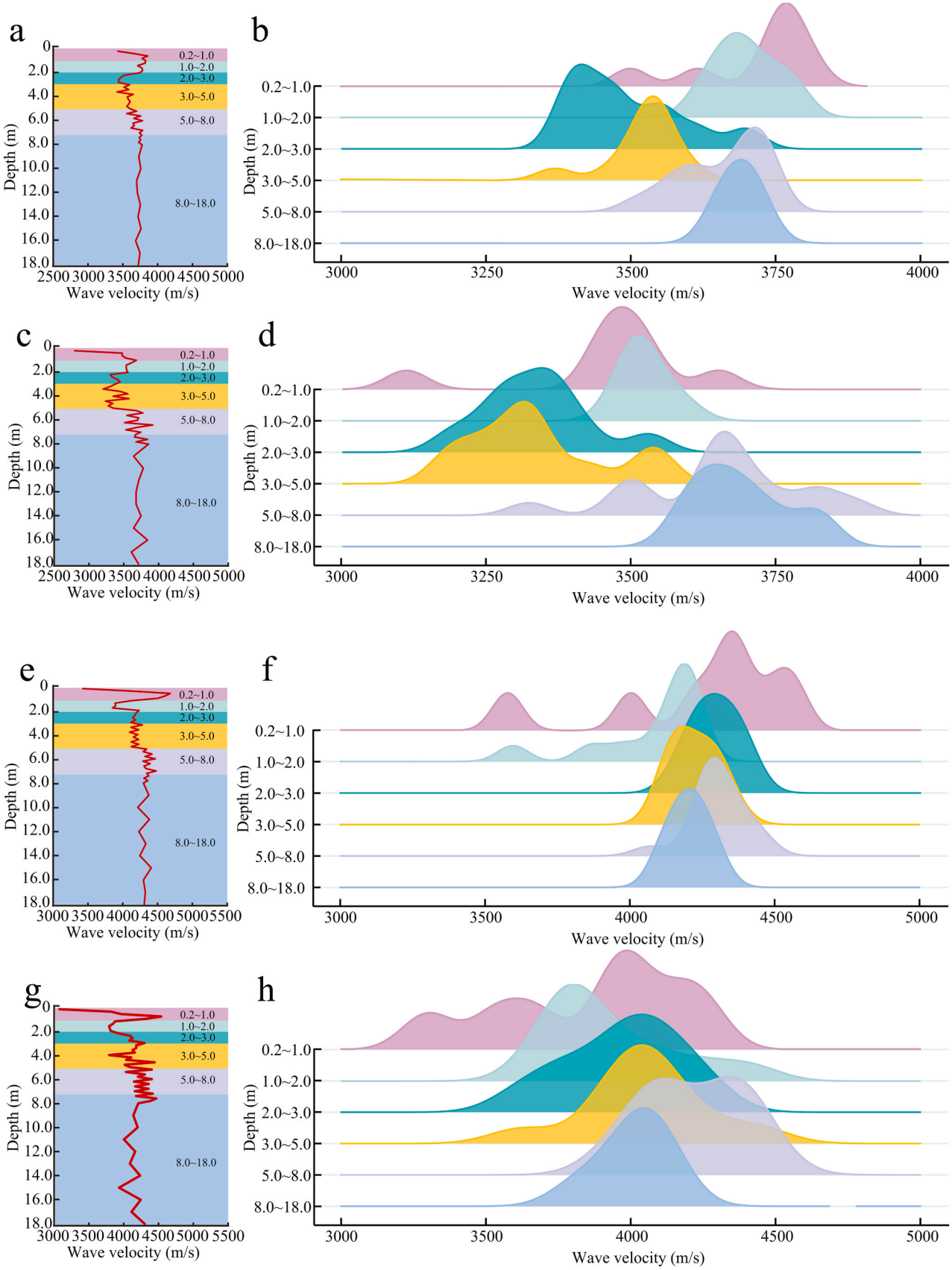

Fig. 6. "Plane" monitoring results: (a),(e) Wave velocity curve of upstream and downstream side wall before collapse; (c),(g) Wave velocity curve of upstream and downstream side wall after collapse; (b),(d),(f),(h) Statistical distribution of wave velocities.

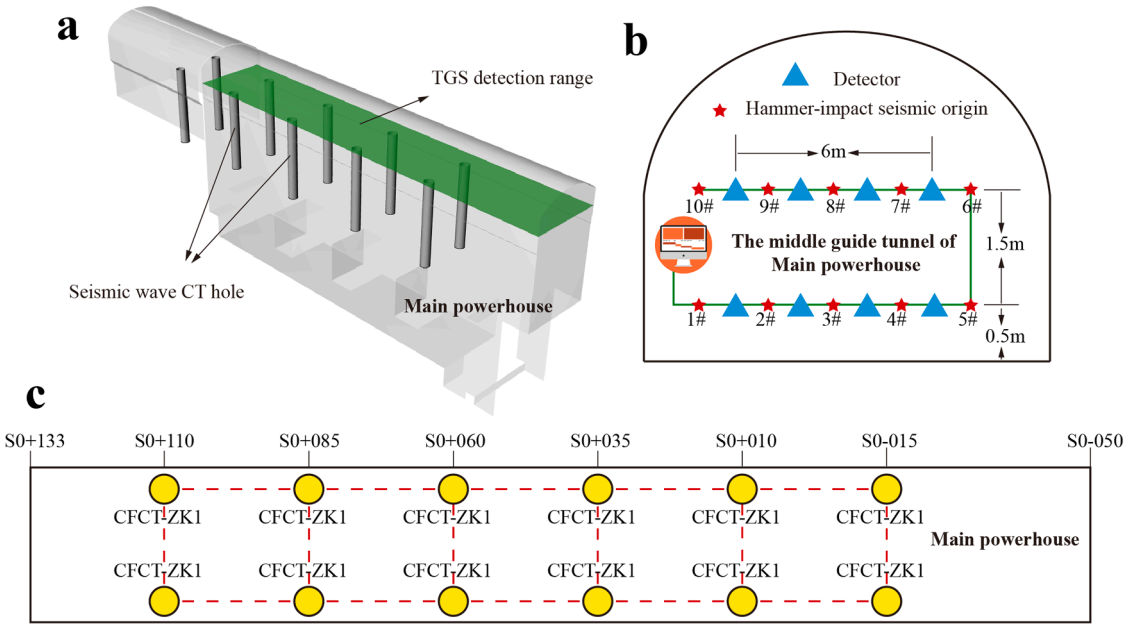

Fig. 7. "Plane" monitoring layout diagram: (a) Advanced geological prediction and seismic wave CT schematic diagram; (b) Sensor arrangement of advanced geological prediction; (c) Seismic wave CT hole layout diagram.

composed mainly of a series of NW-trending folds with roughly parallel scales, and the direction is NW300° to NW330°. No regional fault passes through the dam site area, and small faults and interlayer compression dislocations have developed, as shown in Fig. 3. The F20 fault has a great influence on the main powerhouse, and the fault is gently inclined. The width of the fracture zone is 70–100 cm, and the visible trace length on the surface is more than 90 m. The fault is thick, the mechanical properties are poor, the dip angle is slow, and it passes through the roof arch of the powerhouse, which has a controlling effect on the stability of the surrounding rock of the powerhouse. Under the action of self-weight and tectonic stress, the in situ stress field in the engineering area is obviously affected by topography and fault morphology. The maximum principal stress is 5.8–8.3 MPa, and the direction is between N65~N80E. The intermediate principal stress and the minimum principal stress are between 3.6 and 6.5 MPa and 1.2–4.4 MPa, respectively.

2.2. *Occurrence of roof arch collapse*

In March 2021, the excavation of the middle pilot tunnel on the first floor of the main powerhouse began. During the excavation process, frequent falling blocks occurred at the site, so the safety monitoring of the main powerhouse area was strengthened. In May 2021, the excavation of the middle pilot tunnel was completed, after which the expansion of the upstream and downstream sides was carried out. During the expansion process, the phenomenon of falling blocks was more serious, and the maximum rockfall diameter exceeded 10 cm. Therefore, the support was strengthened. Under the action of strong support, no more serious accidents occurred until approximately 4 a.m. on June 9, 2021, when a large-scale collapse accident occurred suddenly in the working face. In a short period of 5 min, more than 4000 cubic rock masses poured down from the top arch of K0 + 070–K0 + 090, which caused a dump truck and an excavator to be buried, and many supporting facilities were destroyed, which caused serious economic losses. The collapse caused the formation of a pit with a depth of more than 12 m, which resulted in the failure of normal excavation in the following half year, and construction was severely delayed. A schematic diagram of the collapse and the site conditions is shown in Fig. 4.

3. Multidimensional thorough perception system of "point, line, plane, and body"

3.1. *"Point" monitoring method*

The "point" monitoring method involves mainly multipoint displacement meters and bolt stress meters, which are used for discontinuous monitoring in time and space. The multipoint displacement meters and bolt stress meters are arranged in several sections of the underground powerhouse. A set of four-point multipoint displacement meters and anchor stress meters are installed on the sidewall, spandrel and top arch of each section to monitor the deformation and stress changes in the surrounding rock during the excavation of the underground powerhouse.

Fig. 5 shows the monitoring results of the multipoint displacement meter and bolt stress meter for the underground powerhouse. Fig. 5a shows the monitoring result of the multipoint displacement meter at the top arch of collapse section 0 + 96 m, and Fig. 5b shows the change curve of the multipoint displacement meter at the spindle upstream of collapse section 0 + 96 m. The curve of the multipoint displacement meter shows no significant increase, with the average daily displacement increase being much less than 1 mm. Until the last recorded data before the collapse on June 5, the deformation remained low, but in the large-scale collapse event on June 9, the surrounding rock fell off extensively, which damaged the "point" monitoring equipment and rendered it ineffective. Fig. 5c-d show the curves of the multipoint displacement meter and bolt stress meter data for the 0 + 84 m section of the underground powerhouse for approximately one year after the collapse. During the monitoring period, the monitoring data revealed a significant step-like increase. The displacement meter at the end of May and the end of June revealed that the deformation was close to 10 mm in one week, and the corresponding stress increased suddenly before that. After this phenomenon occurred at the construction site, the construction progress slowed, and the stress and displacement of the surrounding rock tended to be stable after the support was strengthened.

The above analysis reveals that the "point" monitoring method is not sensitive to sudden disasters such as collapse. The identification of the

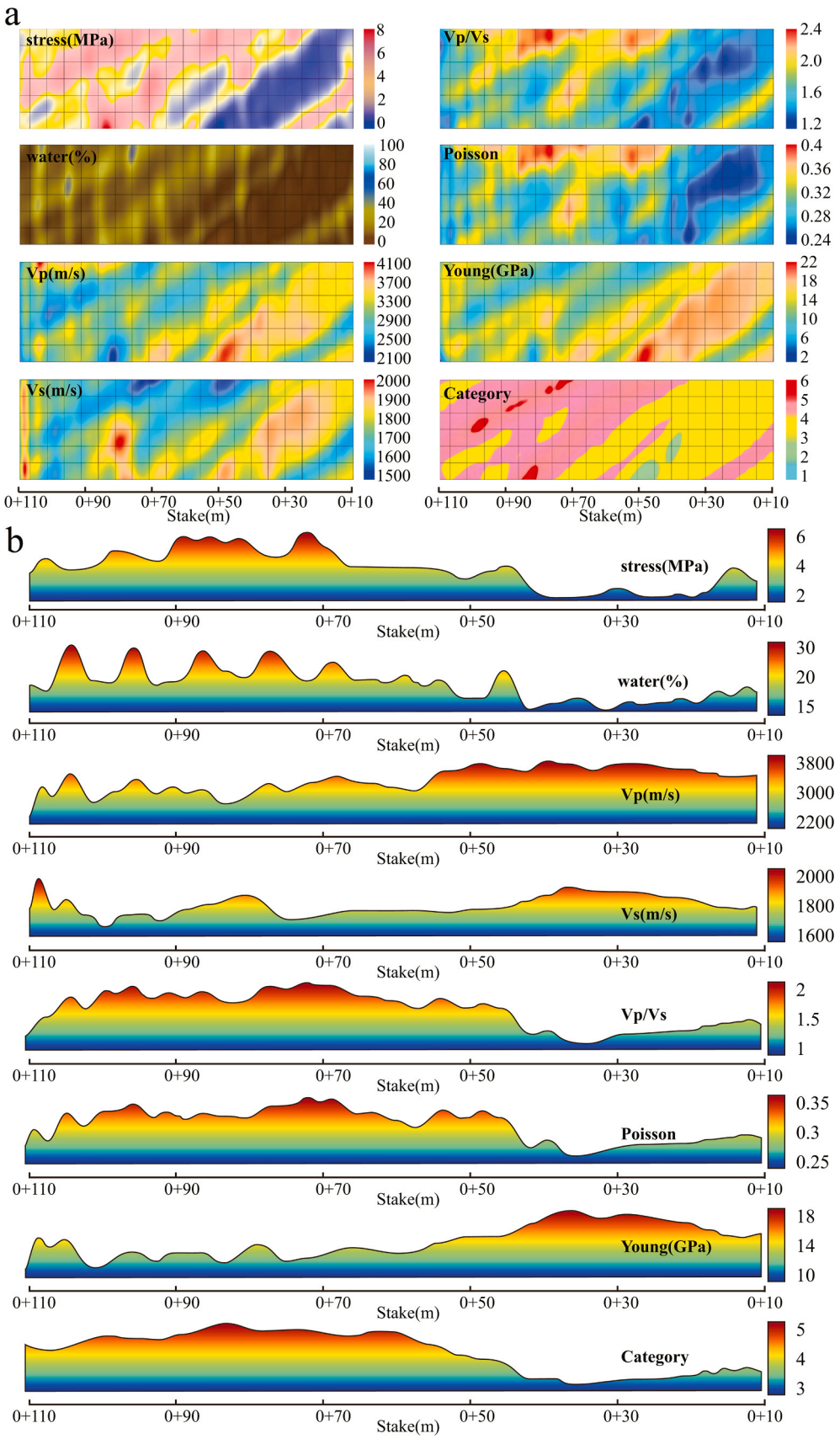

Fig. 8. Advanced geological prediction results of the first floor of powerhouse: (a) Geological information of horizontal plane ahead of the working face; (b) Geological information along the central axis ahead of the working face.

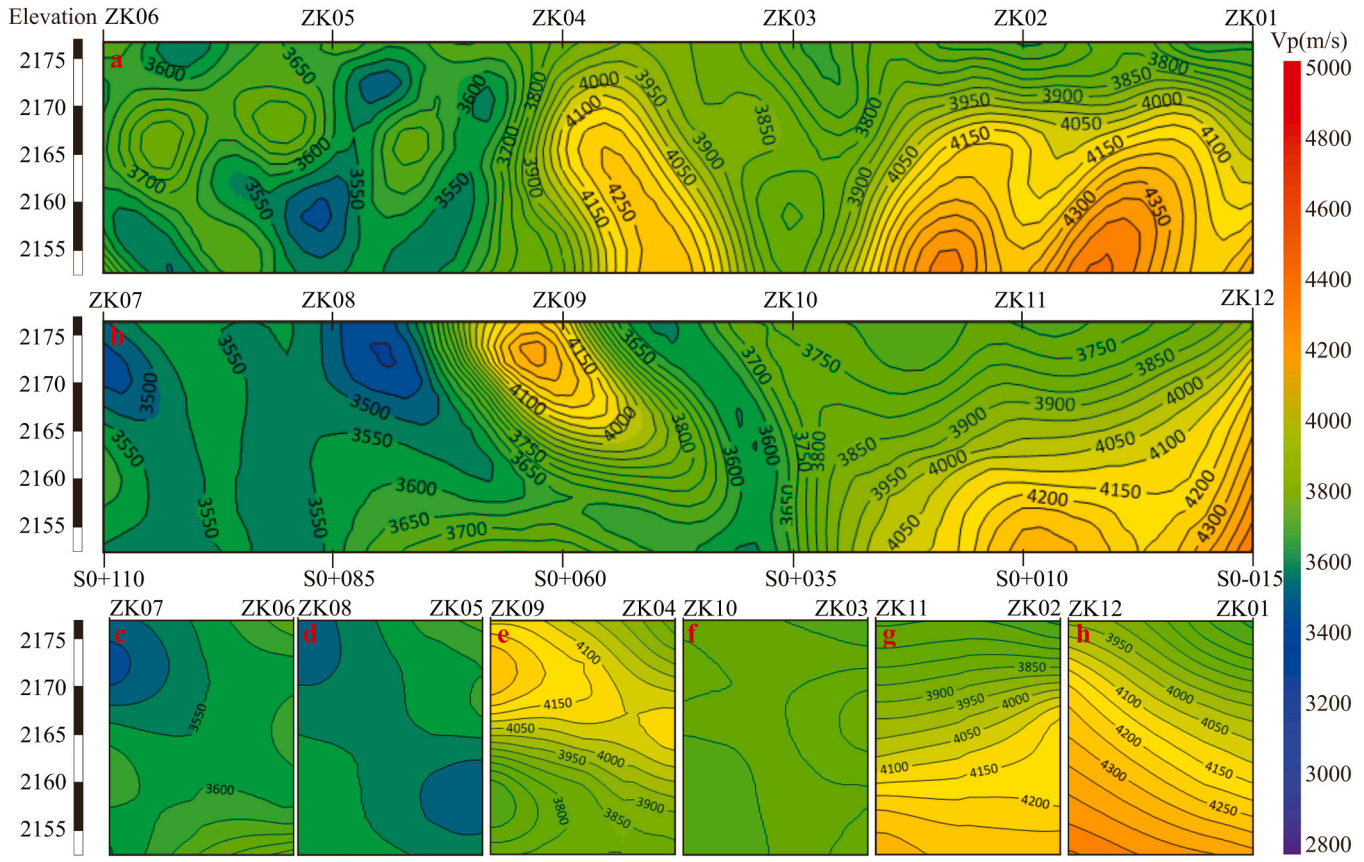

Fig. 9. Seismic wave CT results.

Table 1
Relationship between the surrounding rock integrity coefficient and the surrounding rock state.

Kv	> 0.75	0.75–0.55	0.55–0.35	0.35–0.15	< 0.15
Integrity of the rock mass	Complete	Relatively complete	Relatively broken	Broken	Extremely broken

macroscopic failure phenomenon of surrounding rock with slow deformation and stress growth is relatively accurate, and point monitoring equipment is convenient to install and low in cost, so it should be deployed for conventional monitoring in the construction process of underground engineering.

3.2. *"Line" monitoring method*

The line monitoring method refers to linear continuous monitoring in space, such as acoustic wave monitoring of surrounding rock and monitoring by borehole television. By measuring the propagation velocity and attenuation of acoustic waves in a rock mass, the integrity of the rock mass, the degree of fracture development, the stability of the surrounding rock and the range of the loose circle of surrounding rock can be inferred. Borehole TV monitoring data can directly reflect the lithology and crack development in a borehole. A total of 6 monitoring sections were arranged in the underground powerhouse of the Jinchuan hydropower station. Each monitoring section was arranged with 18 m deep acoustic monitoring holes in the top arch, spandrel and sidewalls. Monitoring was carried out once a week to determine whether the surrounding rock reached a stable state.

Fig. 6 shows the acoustic wave monitoring results for the underground powerhouse at the Jinchuan hydropower station. Fig. 6(a and e) shows the wave velocity curves of the upstream and downstream sidewalls of the main powerhouse at 0 + 85 m one week before the collapse, and Fig. 6(c and g) shows the wave velocity curves of the upstream and downstream sidewalls of the main powerhouse at 0 + 85 m one week after the collapse. The wave velocity distribution of the surrounding rock was statistically analysed, and the wave velocity distribution range of the surrounding rock at each depth was obtained, as shown in Fig. 6 (b, d, f, and h). The figure shows that the wave velocity of the shallow surrounding rock on the upstream side at 0 + 85 m decreased significantly after the collapse, and the wave velocity was not much different at depths greater than 5 m from that at the free surface. Therefore, the

Table 2
Integrity of surrounding rock at the underground powerhouse.

Upstream/Downstream	Stake (m)	Elevation (m)	Vp (m/s)	Kv	Intactness of the rock mass
Upstream	0 + 95–0 + 105	2174–2177	3400–3550	0.44–0.49	Relatively broken
Upstream	0 + 100–0 + 108	2152–2159	3450–3550	0.47–0.49	Relatively broken
Upstream	0 + 82–0 + 90	2155–2160	2956–3400	0.34–0.45	Relatively broken~broken
Upstream	0 + 75–0 + 85	2167–2175	3121–3400	0.38–0.45	Relatively broken
Downstream	0 + 105–0 + 110	2167–2175	3150–3400	0.39–0.45	Relatively broken
Downstream	0 + 74–0 + 86	2168–2177	2949–3450	0.34–0.47	Relatively broken~broken

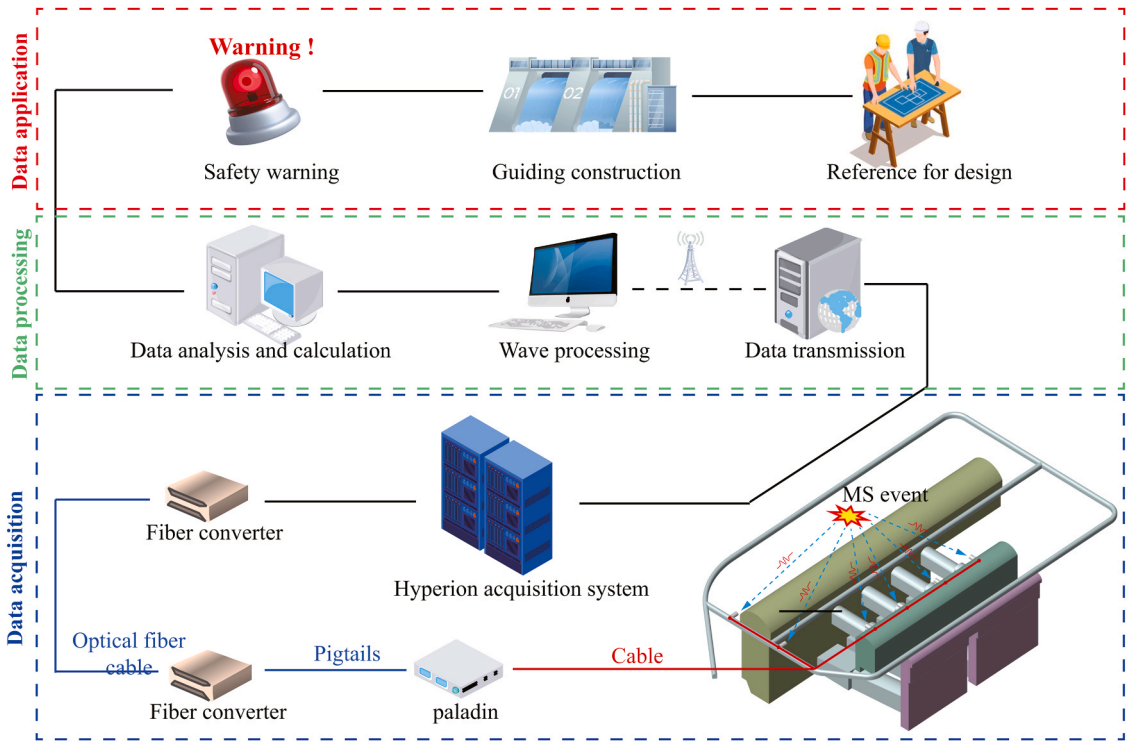

Fig. 10. The topology of the MS monitoring system.

deterioration depth of the upstream surrounding rock caused by the collapse was approximately 5 m. Correspondingly, there was no significant difference in wave velocity when the downstream hole at 0 + 85 m was close to 18 m, so the deterioration depth of the surrounding rock on the downstream side of the collapse section was approximately 18 m. According to the above analysis, the length of the upstream side bolt should exceed 5 m when the collapse section is treated, and the length of the downstream side bolt should exceed 18 m to ensure the stability of the surrounding rock during the collapse treatment.

Another function of "line" monitoring is to determine whether the surrounding rock is in a stable state. When the difference in the acoustic wave velocity between two consecutive times is less than 5 % and the borehole TV shows that the crack does not expand and that no new crack occurs, the surrounding rock is considered to reach a stable state after support, and the next operation can be carried out at this time.

3.3. *"Plane" monitoring method*

The "plane" monitoring method proposed in this paper refers to advanced geological prediction and seismic wave CT. The geological prediction range and acoustic hole layout of seismic waves are shown in Fig. 7a. On the basis of the principle of wave reflection, advanced geological prediction can identify adverse geological features within a range of 5–200 m ahead of the working face. This method involves calculating the physical and mechanical parameters of the rock mass, such as the stress, P-wave and S-wave velocities, Poisson's ratio, and Young's modulus; inverting the risk level of the rock mass; and then evaluating the stability of the unexcavated rock mass ahead. The TGS 360 Pro technology was introduced into the Jinchuan hydropower station. After the formation of the working face on the first floor of the underground powerhouse, the geophone shown in Fig. 7b was positioned at 0 + 110 m to detect the geological information ahead of the working face. Seismic wave CT, which is also known as tomography technology, uses seismic waves to view a rock mass. The rock mass internal structure is imaged by inversion calculations of the seismic wave travel time and attenuation. After excavating the first layer, a seismic wave CT hole with a vertical depth of 25 m can be laid, as shown in Fig. 7c. Since the depth of a single detection is 25 m, another seismic wave CT study needs to be conducted every time the powerhouse is excavated approximately 20 m downwards.

Fig. 8 shows the advanced geological prediction results for the first floor of the powerhouse, Fig. 8a shows the geological information of the horizontal plane ahead of the working face, and Fig. 8b shows the geological information in the direction of the powerhouse central axis ahead of the working face. As shown in the figure, in the range of 0 + 10 m–0 + 60 m, the stress of the surrounding rock changed minimally, the water content was low, the change rate of the wave velocity was low, the P wave velocity was 3300–4100 m/s, the S wave velocity was 1700–1900 m/s, the average Young's modulus was 18.3 GPa, and the risk level was 2.9–3.3. However, in the range of 0 + 60–0 + 100 m, the stress increased significantly; the water content was 20–30 %; the P-wave and S-wave velocities decreased significantly, which indicated that the integrity of the rock mass decreased; the Young's modulus decreased to 12.5 GPa; and the danger level was 4–5. In this range, the rock mass quality and surrounding rock stability were poor, and there was a possibility of a large collapse after excavation.

Fig. 9 shows the seismic wave CT results. The wave velocity in the range of 0 + 60–0 + 110 m was significantly lower than that in the range of 0–15~0 + 30 m, and the lowest wave velocity of 0 + 85 m/s was less than 3000 m/s. The rock mass integrity coefficient Kv is the square of the ratio of the rock mass p-wave velocity to the rock P-wave velocity. The higher Kv is, the more complete the surrounding rock. Table 1 shows the relationship between the surrounding rock integrity coefficient and the surrounding rock state. The average wave velocity of rock in the laboratory was 5026 m/s. According to Fig. 9 and Table 1, the unexcavated rock mass below the first floor of the underground powerhouse was analysed, and the areas with poor rock integrity are shown in Table 2. Table 2 shows that within the elevation range of 2152–2177 m, the rock mass from 0 + 74–0 + 110 m was broken, which posed safety risks for the subsequent excavation process and thus was regarded as a key monitoring object. In the range of 0–15–0 + 74 m, the wave velocity of the rock mass was basically above 4000, and Kv was

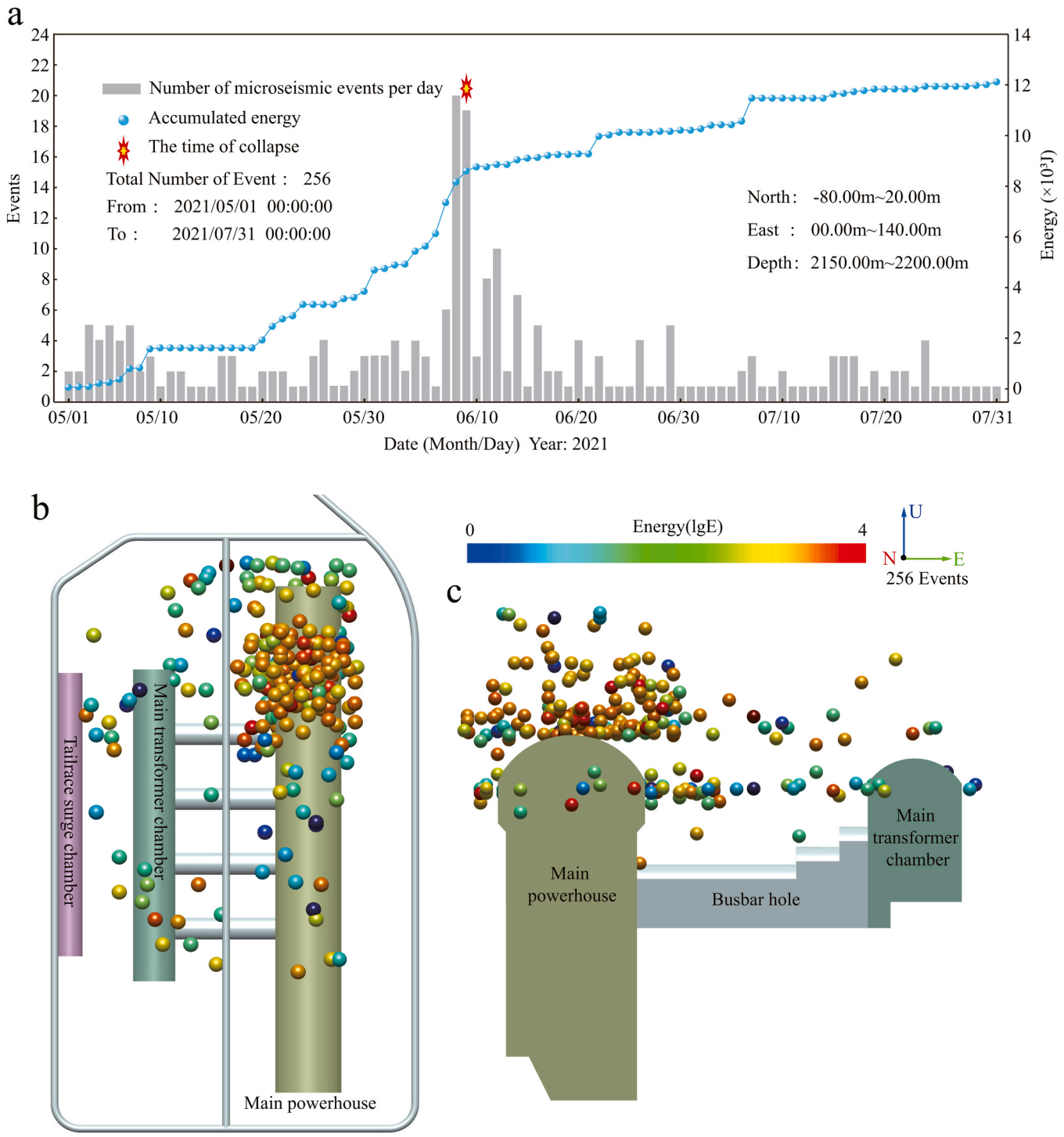

Fig. 11. Spatial and temporal distribution of MS events: (a) MS events and cumulative released energy vs. time; (b) Spatial distribution of MS events.

greater than 0.55, which indicates that the rock mass was relatively complete.

3.4. *"Body" monitoring method*

According to the potential risk area delineated by "plane" monitoring, the body monitoring method of MS monitoring was used to continuously monitor the underground powerhouse of the Jinchuan hydropower station for 24 h, and the elastic waves released during the germination, expansion and penetration of microcracks in the rock mass were collected in real time to automatically invert and calculate the seismological parameters. The topology of the MS monitoring system is shown in Fig. 10. The system consists of three main parts: a data acquisition part, a data processing part, and a data application part. The data acquisition part is composed of an MS acceleration sensor, a data acquisition instrument and a storage host and is responsible for collecting and storing microfracture information. The data processing part mainly performs MS waveform recognition, noise reduction and location, and source parameter calculation. In the data application part, early warning of abnormal source parameters is carried out to guide the construction and provide a reference for support design.

Fig. 11 shows the spatial and temporal distributions of MS events. As

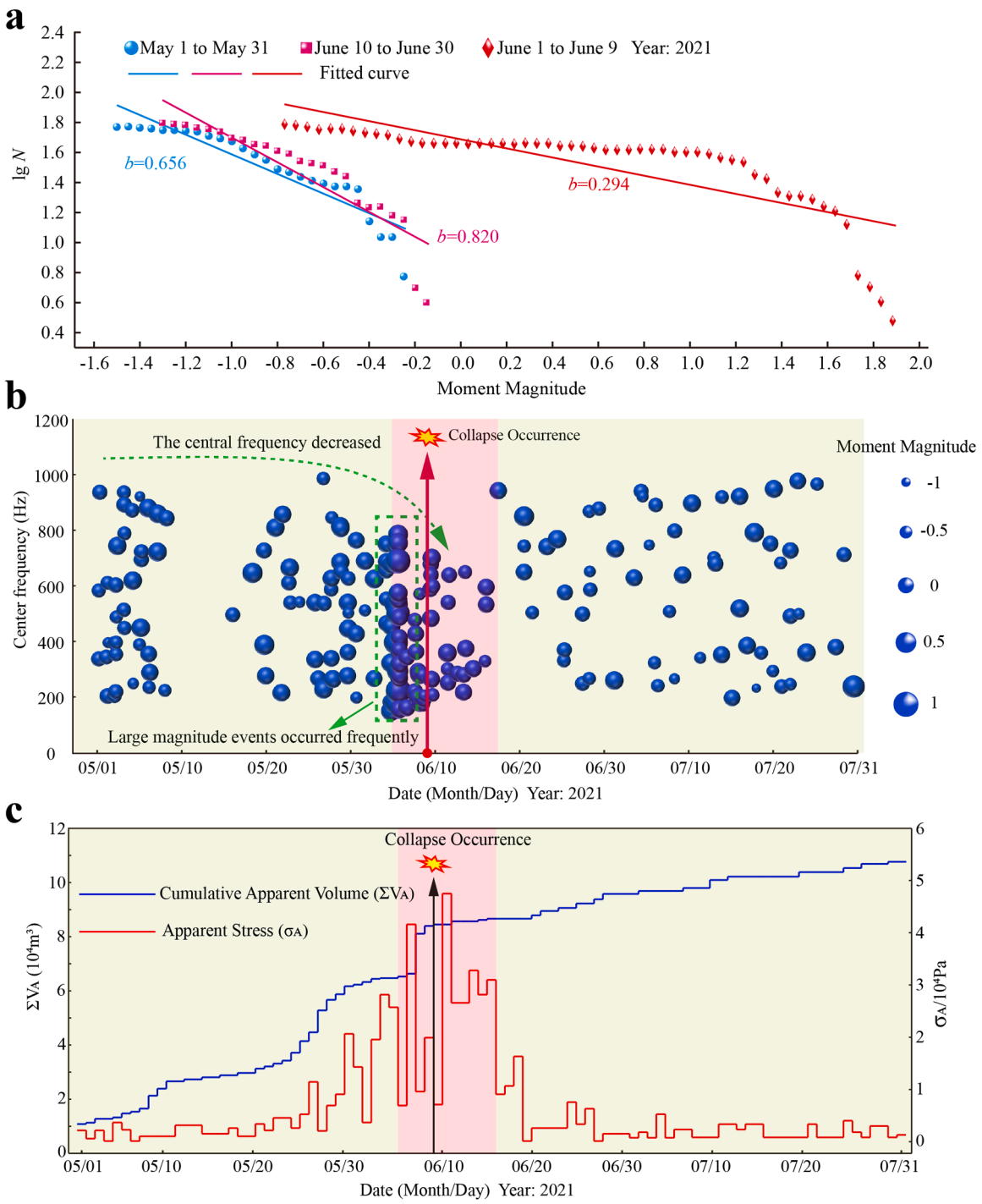

Fig. 12. Evolution law of MS source parameters: (a) b-value; (b) Center frequency; (c) Apparent stress and apparent volume.

shown in Fig. 11a, a total of 256 MS events were triggered during the period from May 1 to June 31, 2021. During May, the frequency of MS events was low, the number of MS events per day was 1–4, and the accumulated energy of the MS events increased slowly. At the beginning of June, the number of MS events began to increase gradually. From June 6 to June 8, the number of MS events increased sharply to 20 per day, and the cumulative energy of the MS events also increased steeply. According to the spatial distribution of MS events in Fig. 11b-c, the MS events were concentrated from 0 + 70–0 + 90 m near the roof arch of the underground powerhouse. An early warning bulletin was issued immediately, and blasting excavation was stopped immediately at the site to reduce the number of personnel who were entering and leaving the underground powerhouse. The fieldwork focused only on the slag discharge operation of the rock mass after the previous blasting. After some time, a large-scale collapse accident occurred in the roof arch of the factory building in the early morning of June 9. Fortunately, owing to the early warning of the collapse, the progress of the operation slowed, there were fewer workers on the working face, and they all took shelter smoothly. This accident did not cause any casualties. Since then, owing to the release of stress, the number of MS events and the cumulative energy of MS events have gradually decreased. Finally, after the "point" monitoring showed that the internal displacement and stress of the surrounding rock had no obvious changes, the "line" monitoring showed that there was no difference in the two consecutive acoustic

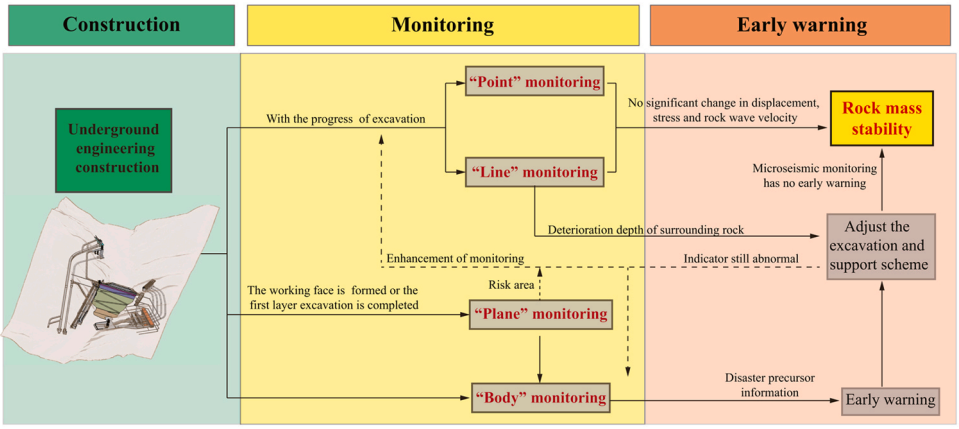

Fig. 13. Multidimensional thorough perception system.

wave velocities; thus, the surrounding rock is considered to be stable, and the next step of collapse treatment can be carried out.

On the basis of the collapse accident, the precursory information of the MS source parameters before the disaster was further refined to provide more accurate guidance for subsequent excavation. In this work, an analysis of the variation laws of the source parameters before and after collapse revealed that the MS b value, MS centre frequency, MS apparent stress, and MS apparent volume can be used as precursor information for disaster occurrence, as shown in Fig. 12. The calculation and physical meanings of the corresponding seismic source parameters are described in detail in Mao et al. [46] and are not repeated here. During May before the collapse, the b value was 0.656, and the b value decreased to 0.294 at the beginning of June, which was a decrease of 56 %. After the collapse, the b value increased again to 0.820. The MS centre frequency can characterize the size of the fracture scale, and a smaller centre frequency corresponds to a larger fracture scale. The evolution law of the centre frequency is similar to that of the b value. When the surrounding rock is stable, the distribution range of the centre frequency is wide and ranges from 200–1000 Hz. Before the collapse, many large-magnitude and low-frequency MS events occurred intensively. After the collapse, the central frequency presented a uniform distribution of high- and low-frequency bands. Apparent stress and apparent volume are also important parameters in MS monitoring. Before the end of May, the MS apparent stress fluctuated among lower values, and the cumulative apparent volume increased slowly. At the beginning of June, the apparent stress increased suddenly, then decreased suddenly, and subsequently suddenly rose to a relatively high value and then decreased again. The cumulative apparent volume experienced significant jump growth on June 7, followed by a collapse. After the collapse, the apparent volume gradually decreased to a lower value after reaching its peak on June 10, and the cumulative apparent volume also slowly increased.

On the basis of the above analysis, the precursor warning indications before a disaster of surrounding rock are as follows: the number of MS events, cumulative energy and magnitude suddenly increase; the b value and centre frequency decrease; the apparent stress suddenly increases to a large value and then suddenly decreases; and the cumulative apparent volume increases steeply. According to the precursory information, surrounding rock disasters can be predicted more accurately. If two or more of these precursor indications occur, a quick warning bulletin can be issued immediately on site for early warning. MS monitoring is a 24-hour online monitoring method that can detect precursor information first and then ensure the timeliness of early warnings.

3.5. *Multidimensional thorough perception system*

The above section analyses the point, line, plane, and body monitoring methods. However, the monitoring methods of different dimensions are not independent of each other but cooperate to ensure the safety and stability of the entire underground cavern group. Each monitoring method interacts to form a multidimensional thorough perception system, as shown in Fig. 13. With the excavation of underground engineering, “point” and “line” monitoring methods are carried out as excavation progresses to monitor the internal stress, deformation and crack development of the surrounding rock. When the working face is formed or the excavation of the first layer is completed, "plane" monitoring is carried out; that is, geological prediction of the rock mass ahead of the working face is carried out by TGS 360 Pro technology. Seismic wave CT is used to detect vertical unexcavated rock masses. The rock mass risk area revealed by “plane” monitoring is taken as the core area of “body” monitoring, and an MS monitoring system is established. When MS monitoring indicates the occurrence of a disaster precursor, early warning is immediately carried out. The excavation and support scheme is adjusted according to the damage depth of the surrounding rock by “line” monitoring. If the MS source parameters are still abnormal for a long time after the scheme is adjusted, the monitoring will continue to be strengthened, and the construction scheme will continue to be adjusted until the source parameters are within normal values. At this time, if “point” and “line” monitoring reveals that the stress, deformation, and wave velocity of the surrounding rock do not fluctuate, the surrounding rock can be proven to recover to a stable state after the construction scheme is adjusted, and then the next excavation operation can be carried out.

4. Application of the multidimensional system in the surge chamber

The height—width ratio of the surge chamber of the Jinchuan hydropower station reaches 5:1, which is a typical ratio for a high-elevation underground cavern. In addition, the surrounding rock of the surge chamber is relatively broken, which easily causes deformation and failure of the surrounding rock during excavation. Therefore, a multidimensional "point, line, plane, and body" perception system was established in the surge chamber to monitor the state of the surrounding rock during excavation unloading.

Fig. 14 shows the excavation and monitoring of the surge chamber. The first layer excavation of the surge chamber was completed on July 1, 2021, and then seismic wave CT was carried out on the vertical unexcavated rock mass on July 15. The results revealed that the wave velocity of the rock mass between 0 + 10–0 + 25 m was relatively low and that the rock mass quality was poor. On this basis, 0 + 10–0 + 25 m was taken as the core monitoring position, and an MS monitoring system was deployed on August 1, as shown in Fig. 14. "Point and line" monitoring was carried out continuously throughout the excavation process. In July

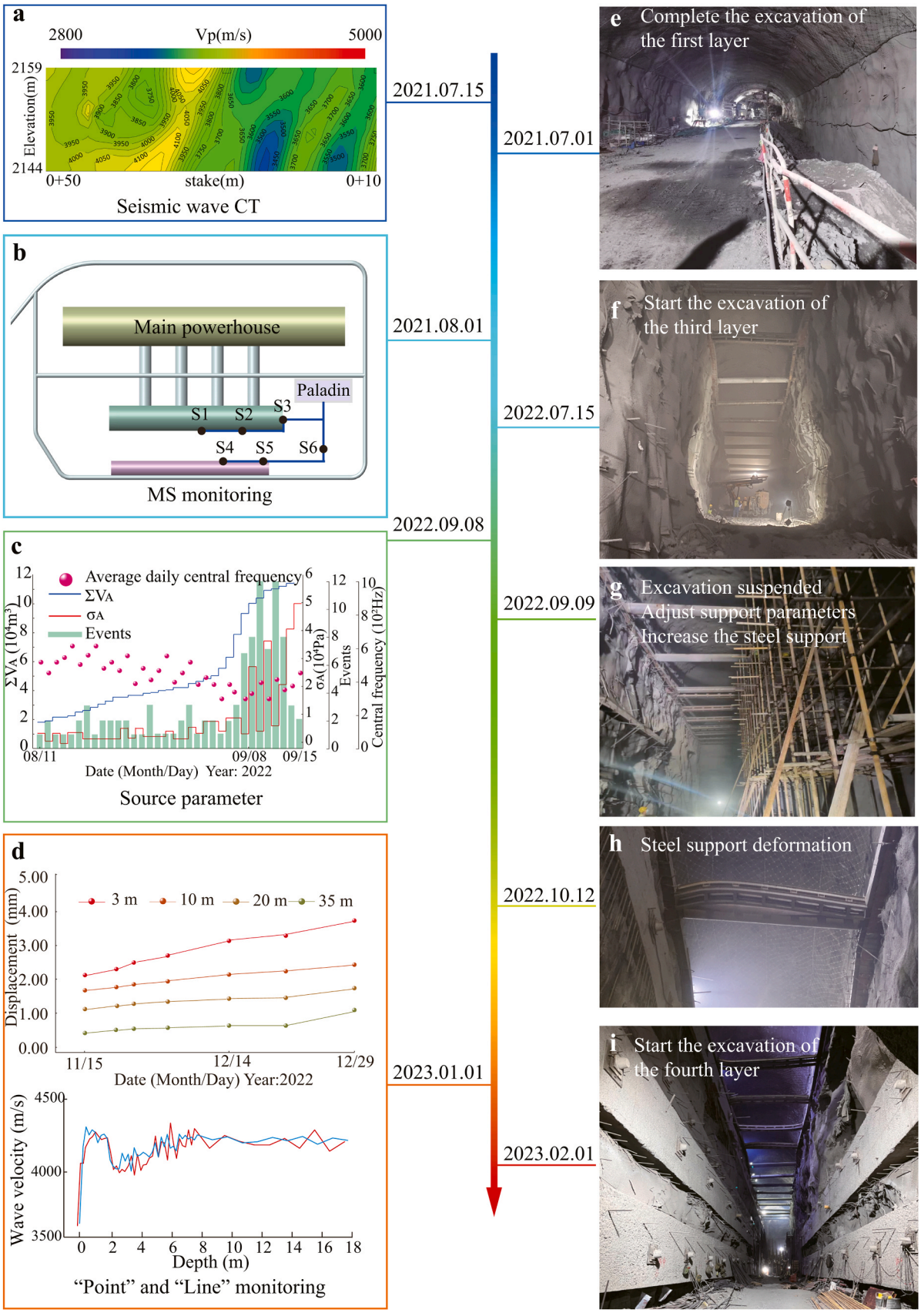

Fig. 14. Excavation and monitoring of the surge chamber.

2022, the excavation of the third layer of the surge chamber began. In September, the MS source parameters showed that the number of MS events, MS energy, and cumulative apparent volume increased sharply; the daily average centre frequency showed a downwards trend; the apparent stress decreased suddenly after a sudden increase; and the MS events occurred at approximately 0 + 20 m. Combined with the precursor information of the surrounding rock disaster described in 3.4, a risk of surrounding rock disaster near the surge chamber at 0 + 20 m was inferred, and an early warning bulletin was sent immediately. The construction and design units attached great importance to the bulletin, and they adjusted the support scheme in time on September 9, strengthened the steel support, and stopped the excavation immediately. On October 12, the steel support deformed significantly, which indicated that the steel support effectively prevented the instability of the sidewall.

On January 1, 2023, the monitoring data revealed that there was no significant change in the performance of the multipoint displacement meter, bolt stress meter, or acoustic wave monitoring within one month, and no MS early warning precursor information appeared. The surrounding rock was considered to have reached a basically stable state, so the excavation of the surge chamber resumed on February 1, 2023. The surrounding rock instability did not occur again in the subsequent excavation process.

Therefore, the “point, line, plane, and body” multidimensional thorough perception system successfully warned of the deformation of the surrounding rock at the surge chamber, effectively prevented a disaster of the surrounding rock, and ensured the safety of life and property.

5. Conclusions

On the basis of the underground cavern of the Jinchuan hydropower station, a multidimensional thorough perception system was constructed through conventional monitoring methods, advanced geological prediction technology and MS monitoring technology, and the significance of each monitoring method was analysed. The precursory early warning information for the surrounding rock disaster was identified according to the collapse of the top arch at the main powerhouse. The multidimensional system was successfully adopted for the surge chamber. The following main conclusions can be drawn.

(1) A multidimensional perception system of type "point, line, plane, and body" for underground caverns at the Jinchuan hydropower station was established. A multipoint displacement meter, a bolt stress meter and acoustic wave monitoring were used as “point and line” monitoring methods to monitor the stress, strain and crack development characteristics of the surrounding rock. A TGS 360 Pro system and seismic wave CT were used as "plane" monitoring methods to reveal the poor geological features of the surrounding rock. The "body" monitoring method, namely, MS monitoring, was adopted to delineate the potential risk areas identified by "plane" monitoring, and early warning of surrounding rock disasters was carried out during excavation. The monitoring methods of each dimension jointly determined whether the surrounding rock was in a stable state.

(2) Precursor information for the surrounding rock disaster was obtained. On the basis of the collapse of the top arch in the main powerhouse, the MS precursory information for the surrounding rock disaster can be summarized as follows: the number of MS events, cumulative energy and magnitude suddenly increased; the b value and central frequency decreased; the apparent stress suddenly increased to a larger value and then suddenly decreased; and the cumulative apparent volume increased steeply.

(3) A multidimensional system was successfully adopted for the surge chamber. With respect to the deformation of the surrounding rock in the surge chamber, the multidimensional thorough perception system of type "point, line, plane, body" was used to successfully forecast the surrounding rock deformation and prevent possible disasters. This successful application will help extend the multidimensional monitoring system to other similar underground engineering applications.

CRediT authorship contribution statement

Haoyu Mao: Writing – original draft. **Nuwen Xu:** Funding acquisition, Writing – review & editing. **Peiwei Xiao:** Methodology. **Xiang Zhou:** Software. **Xinchao Ding:** Formal analysis. **Biao Li:** Writing – review & editing.

Funding

This work was supported by the National Natural Science Foundation of China (Grant No. U23A2060, 42177143, 42277461).

Declaration of Competing Interest

The authors declare that they have no known competing financial interests or personal relationships that could have appeared to influence the work reported in this paper.

References

[1] Z.J. Liu, C.Q. Zhang, C.S. Zhang, et al., Deformation and failure characteristics and fracture evolution of cryptocrystalline basalt, J. Rock Mech. Geotech. Eng. 11 (2019) 990–1003, https://doi.org/10.1016/j.jrmge.2019.04.005.
[2] H.Y. Mao, N.W. Xu, X. Li, et al., Analysis of rockburst mechanism and warning based on microseismic moment tensors and dynamic Bayesian networks, J. Rock Mech. Geotech. Eng. 15 (2023) 2521–2538, https://doi.org/10.1016/j.jrmge.2022.12.005.
[3] Q.C. Sun, S.J. Li, H.S. Guo, et al., In situ test of excavation damaged zone of columnar jointed rock masses under different borehole conditions, Bull. Eng. Geol. Environ. 80 (2021) 2991–3007, https://doi.org/10.1007/s10064-020-02100-6.
[4] Q.H. Qian, X.P. Zhou, Failure behaviors and rock deformation during excavation of underground Cavern group for Jinping I hydropower station, Rock Mech. Rock Eng. 51 (2018) 2639–2651, https://doi.org/10.1007/s00603-018-1518-x.
[5] D.-F. Chen, X.-T. Feng, D.-P. Xu, et al., Use of an improved ANN model to predict collapse depth of thin and extremely thin layered rock strata during tunnelling, Tunn. Undergr. Space Technol. 51 (2016) 372–386, https://doi.org/10.1016/j.tust.2015.09.010.
[6] X. Ding, X. Niu, Q. Pei, et al., Stability of large underground caverns excavated in layered rock masses with steep dip angles: A case study, Bull. Eng. Geol. Environ. 78 (2019) 5101–5133, https://doi.org/10.1007/s10064-018-01440-8.
[7] A. Li, N. Xu, F. Dai, et al., Stability analysis and failure mechanism of the steeply inclined bedded rock masses surrounding a large underground opening, Tunn. Undergr. Space Technol. 77 (2018) 45–58, https://doi.org/10.1016/j.tust.2018.03.023.
[8] D.-P. Xu, X.-T. Feng, D.-F. Chen, et al., Constitutive representation and damage degree index for the layered rock mass excavation response in underground openings, Tunn. Undergr. Space Technol. 64 (2017) 133–145, https://doi.org/10.1016/j.tust.2017.01.016.
[9] Y.-Y. Zhou, D.-P. Xu, G.-K. Gu, et al., The failure mechanism and construction practice of large underground caverns in steeply dipping layered rock masses, Eng. Geol. 250 (2019) 45–64, https://doi.org/10.1016/j.enggeo.2019.01.006.
[10] Q. Fan, X. Feng, W. Weng, et al., Unloading performances and stabilizing practices for columnar jointed basalt: A case study of Baihetan hydropower station, J. Rock Mech. Geotech. Eng. 9 (2017) 1041–1053, https://doi.org/10.1016/j.jrmge.2017.07.003.
[11] Q. Jiang, X.-T. Feng, Y.H. Hatzor, et al., Mechanical anisotropy of columnar jointed basalts: An example from the Baihetan hydropower station, China, Eng. Geol. 175 (2014) 35–45, https://doi.org/10.1016/j.enggeo.2014.03.019.
[12] Q. Qiu, G. Rong, H. Zhang, et al., Investigation on effect evaluation of seepage control system of large underground powerhouse of the Baihetan hydropower station, Tunn. Undergr. Space Technol. 142 (2023) 105429, https://doi.org/10.1016/j.tust.2023.105429.
[13] A. Shi, Y. Wei, Y. Zhang, et al., Study on the strength characteristics of columnar jointed basalt with a true triaxial apparatus at the Baihetan hydropower station, Rock Mech. Rock Eng. 53 (2020) 4947–4965, https://doi.org/10.1007/s00603-020-02195-z.
[14] A. Shi, C. Li, W. Hong, et al., Comparative analysis of deformation and failure mechanisms of underground powerhouses on the left and right banks of Baihetan hydropower station, J. Rock Mech. Geotech. Eng. 14 (2022) 731–745, https://doi.org/10.1016/j.jrmge.2021.09.012.

[15] J.-S. Zhao, B.-R. Chen, Q. Jiang, et al., In-situ comprehensive investigation of deformation mechanism of the rock mass with weak interlayer zone in the Baihetan hydropower station, Tunn. Undergr. Space Technol. 148 (2024) 105690, https://doi.org/10.1016/j.tust.2024.105690.
[16] J.-S. Zhao, X.-T. Feng, Q. Jiang, et al., Microseismicity monitoring and failure mechanism analysis of rock masses with weak interlayer zone in underground intersecting chambers: A case study from the Baihetan hydropower station, China, Eng. Geol. 245 (2018) 44–60, https://doi.org/10.1016/j.enggeo.2018.08.006.
[17] X.-Y. Liu, D.-P. Xu, Q. Jiang, et al., Excavation response and reinforcement practice of large underground caverns within high-stress hard rock masses: The case of Shuangjiangkou hydropower station, China, Tunn. Undergr. Space Technol. 147 (2024) 105698, https://doi.org/10.1016/j.tust.2024.105698.
[18] R. Xue, Z. Liang, N. Xu, et al., Rockburst prediction and stability analysis of the access tunnel in the main powerhouse of a hydropower station based on microseismic monitoring, Int. J. Rock Mech. Min. Sci. 126 (2020) 104174, https://doi.org/10.1016/j.ijrmms.2019.104174.
[19] R. Xue, Z. Liang, N. Xu, Rockburst prediction and analysis of activity characteristics within surrounding rock based on microseismic monitoring and numerical simulation, Int. J. Rock Mech. Min. Sci. 142 (2021) 104750, https://doi.org/10.1016/j.ijrmms.2021.104750.
[20] E. Hoek, E.T. Brown, Practical estimates of rock mass strength, Int. J. Rock Mech. Min. Sci. 34 (1997) 1165–1186, https://doi.org/10.1016/s1365-1609(97)80069-x.
[21] C.D. Martin, R. Christiansson, Estimating the potential for spalling around a deep nuclear waste repository in crystalline rock, Int. J. Rock Mech. Min. Sci. 46 (2009) 219–228, https://doi.org/10.1016/j.ijrmms.2008.03.001.
[22] M.C. Saceanu, A. Paluszny, R.W. Zimmerman, et al., Fracture growth leading to mechanical spalling around deposition boreholes of an underground nuclear waste repository, Int. J. Rock Mech. Min. Sci. 152 (2022) 105038, https://doi.org/10.1016/j.ijrmms.2022.105038.
[23] T. Makita, Y. Miyanaga, K. Iguchi, et al., Underground oil storage facilities in Japan, Eng. Geol. 35 (1993) 191–198, https://doi.org/10.1016/0013-7952(93)90006-x.
[24] E.-S. Park, S.-K. Chung, Experience and challenge of underground oil/gas storage caverns in Korea, Geosystem Eng. 17 (2014) 294–302, https://doi.org/10.1080/12269328.2014.988300.
[25] G. Zhang, H. Zhang, Y. Liu, et al., Surrounding rock stability of horizontal cavern reconstructed for gas storage, J. Energy Storage 59 (2023) 106534, https://doi.org/10.1016/j.est.2022.106534.
[26] A. Haack, Current safety issues in traffic tunnels, Tunn. Undergr. Space Technol. 17 (2002) 117–127, https://doi.org/10.1016/s0886-7798(02)00013-5.
[27] W. Liu, J. Chen, L. Chen, et al., Deformation evolution and failure mechanism of monoclinic and soft-hard interbedded strata: Study of Muzhailing tunnel, J. Perform. Constr. Facil 35 (2021) 04021042, https://doi.org/10.1061/(asce)cf.1943-5509.0001605.
[28] W. Pan, Z. Gao, C. Zheng, et al., Analysis on the influence of cross tunnel construction on the deformation of the existing high-speed railway tunnel, Geotech. Geol. Eng. 36 (2018) 4001–4013, https://doi.org/10.1007/s10706-018-0553-4.
[29] K.-I. Song, G.-C. Cho, S.-B. Chang, Identification, remediation, and analysis of karst sinkholes in the longest railroad tunnel in South Korea, Eng. Geol. 135-136 (2012) 92–105, https://doi.org/10.1016/j.enggeo.2012.02.018.
[30] S. Li, M. Gao, X. Yang, et al., Numerical simulation of spatial distributions of mining-induced stress and fracture fields for three coal mining layouts, J. Rock Mech. Geotech. Eng. 10 (2018) 907–913, https://doi.org/10.1016/j.jrmge.2018.02.008.
[31] M. He, Q. Wang, Q. Wu, Innovation and future of mining rock mechanics, J. Rock Mech. Geotech. Eng. 13 (2021) 1–21, https://doi.org/10.1016/j.jrmge.2020.11.005.
[32] H. Kang, F. Gao, G. Xu, et al., Mechanical behaviors of coal measures and ground control technologies for China's deep coal mines – a review, J. Rock Mech. Geotech. Eng. 15 (2023) 37–65, https://doi.org/10.1016/j.jrmge.2022.11.004.
[33] C. Xie, H. Nguyen, X.-N. Bui, et al., Predicting roof displacement of roadways in underground coal mines using adaptive neuro-fuzzy inference system optimized by various physics-based optimization algorithms, J. Rock Mech. Geotech. Eng. 13 (2021) 1452–1465, https://doi.org/10.1016/j.jrmge.2021.07.005.
[34] G. Cheng, W. Xu, B. Shi, et al., Experimental study on the deformation and failure mechanism of overburden rock during coal mining using a comprehensive intelligent sensing method, J. Rock Mech. Geotech. Eng. 14 (2022) 1626–1641, https://doi.org/10.1016/j.jrmge.2022.07.016.
[35] G.G. Xu, G.Y. Ma, Q.B. Li, et al., Underground excavation in Xiaolangdi project in Yellow River, Eng. Geol. 76 (2004) 129–139, https://doi.org/10.1016/j.enggeo.2004.06.010.
[36] W.S. Zhu, X.J. Li, Q.B. Zhang, et al., A study on sidewall displacement prediction and stability evaluations for large underground power station caverns, Int. J. Rock Mech. Min. Sci. 47 (2010) 1055–1062, https://doi.org/10.1016/j.ijrmms.2010.07.008.
[37] Z.-S. Wang, Y. Li, W.-S. Zhu, et al., Field monitoring of splitting failure for surrounding rock masses and applications of energy dissipation model, Geomech. Eng. 12 (2017) 595–609, https://doi.org/10.12989/gae.2017.12.4.595.
[38] B. Li, Q.-F. Ding, N.-W. Xu, et al., Characteristics of microseismic b-value associated with rock mass large deformation in underground powerhouse caverns at different stress levels, J. Cent. South Univ. 29 (2022) 693–711, https://doi.org/10.1007/s11771-022-4946-4.
[39] B. Li, N. Xu, P. Xiao, et al., Microseismic monitoring and forecasting of dynamic disasters in underground hydropower projects in southwest China: A review, J. Rock Mech. Geotech. Eng. 15 (2023) 2158–2177, https://doi.org/10.1016/j.jrmge.2022.10.017.
[40] B. Li, N. Xu, F. Dai, et al., Dynamic analysis of rock mass deformation in large underground caverns considering microseismic data, Int. J. Rock Mech. Min. Sci. 122 (2019) 104078, https://doi.org/10.1016/j.ijrmms.2019.104078.
[41] F. Dai, B. Li, N. Xu, et al., Deformation forecasting and stability analysis of large-scale underground powerhouse caverns from microseismic monitoring, Int. J. Rock Mech. Min. Sci. 86 (2016) 269–281, https://doi.org/10.1016/j.ijrmms.2016.05.001.
[42] Y.-X. Xiao, X.-T. Feng, B.-R. Chen, et al., Excavation-induced microseismicity in the columnar jointed basalt of an underground hydropower station, Int. J. Rock Mech. Min. Sci. 97 (2017) 99–109, https://doi.org/10.1016/j.ijrmms.2017.04.012.
[43] Y.-X. Xiao, X.-T. Feng, G.-L. Feng, et al., Mechanism of evolution of stress–structure controlled collapse of surrounding rock in caverns: A case study from the Baihetan hydropower station in China, Tunn. Undergr. Space Technol. 51 (2016) 56–67, https://doi.org/10.1016/j.tust.2015.10.020.
[44] J.-S. Zhao, B.-R. Chen, Q. Jiang, et al., Microseismic monitoring of rock mass fracture response to blasting excavation of large underground caverns under high geostress, Rock Mech. Rock Eng. 55 (2021) 733–750, https://doi.org/10.1007/s00603-021-02709-3.
[45] J.-S. Zhao, Q. Jiang, J.-F. Lu, et al., Rock fracturing observation based on microseismic monitoring and borehole imaging: In situ investigation in a large underground cavern under high geostress, Tunn. Undergr. Space Technol. 126 (2022) 104549, https://doi.org/10.1016/j.tust.2022.104549.
[46] H. Mao, N. Xu, Z. Zhou, et al., Failure mechanism and deformation forecasting of surrounding rock mass in an underground cavern based on engineering analogy method, Tunn. Undergr. Space Technol. 143 (2024) 105497, https://doi.org/10.1016/j.tust.2023.105497.
[47] X. Xue, M. Xiao, Deformation evaluation on surrounding rocks of underground caverns based on PSO-LSSVM, Tunn. Undergr. Space Technol. 69 (2017) 171–181, https://doi.org/10.1016/j.tust.2017.06.019.
[48] X. Li, N. Xu, H. Mao, et al., Deformation characteristics and damage evolution analysis of weak interlayer zone in fractured underground cavern, Tunn. Undergr. Space Technol. 147 (2024) 105686, https://doi.org/10.1016/j.tust.2024.105686.
[49] P.-W. Xiao, X.-G. Yang, B. Li, et al., Roof arch collapse of underground cavern in fractured rock mass: In situ monitoring and numerical modeling, J. Rock Mech. Geotech. Eng. 17 (2025) 2778–2792, https://doi.org/10.1016/j.jrmge.2024.05.018.

Nuwen Xu is a professor of Rock Mechanics and Rock Engineering at Sichuan University. His research interests include (1) numerical simulation analysis of geotechnical engineering; (2) stability evaluation of surrounding rock mass in underground engineering; and (3) the mechanism, monitoring and warning of dynamic disasters in deep rock mass. He is the editorial board members of Journal of Rock Mechanics and Geotechnical Engineering, Tunnelling and Underground Space Technology, Journal of Intelligent Construction, Chinese Journal of Rock Mechanics and Engineering, etc.